Enhanced Procedure for Fabrication of an Ultrahydrophobic Aluminum Alloy Surface using Fatty Acid Modifiers

M. Fallah[a], A. Rabiee[a], M. Ghashghaee[b],* and A. Ershad-Langroudi[c]

[a]*Faculty of Polymer Science, Iran Polymer and Petrochemical Institute, P.O. Box: 14965-115, Tehran, Iran*
[b]*Faculty of Petrochemicals, Iran Polymer and Petrochemical Institute, P.O. Box: 14975-112, Tehran, Iran*
[c]*Faculty of Polymer Processing, Iran Polymer and Petrochemical Institute, P.O. Box: 14965-115, Tehran, Iran*

A superhydrophobic aluminum surface was fabricated through an enhanced low-cost approach and the effects of several relevant factors on static contact angle and sliding angle were investigated. First, the operating parameters including the etching time as well as the reaction time and temperature were varied. Next, the so-called chemical factors including three different fatty acids and five different solvents were examined. The surface was analyzed by means of SEM, ATR-FTIR, EDX and WCA measurements. The results show that the immersion time of about 5 min and the reaction temperature of about 60 °C were the optimum conditions for the creation of a superhydrophobic Al surface with excellent self-cleaning properties. Overall, the choice of oleic acid and ethanol were found to be the best as the fatty acid and solvent, respectively. The highest contact angle was 163.7° and the lowest sliding angle was about 1°.

INTRODUCTION

Fabrication of ultrahydrophobic (superhydrophobic) surfaces has absorbed the attention of several scientists to this field owing to its practical importance [1]. The ultrahydrophobicity has been defined as a property of the surface signified as a high water repellency and high contact angles ($\theta > 150°$) often accompanied with a low water sliding angle ($\theta < 10°$) [2]. The hydrophobicity stems from two surface features including the surface energy and morphology, such that the higher the roughness of the surface and the lower the surface energy, the larger the contact angle [3-4]. On a perfect smooth surface with no covering layer, the static contact angle can amount to ~120° at most. Hence, constructing a suitable micro-structure is the key for obtaining a superhydrophobic surface [5-6]. There exist many of such surfaces in the nature, such as the lotus leaves. To mimic this nature-made self-cleaning property,

various synthetic superhydrophobic surfaces have been built [7]. Superhydrophobic surfaces have obtained several applications, including the self-cleaning, anti-icing, corrosion resistance, anti-biofouling treatments, stain resistance in textiles, friction controlling, reducing the drag resistance of hulls in ships/submarines, microinjection needles, preventing from obstruction of the oil pipes, fog condensation, oil/water separation, *etc*. [4-6,8-14]. Hence, it has been an interesting topic to bestow this property to different solid materials.

Thanks to their high strength, very good electrical and heat conductivities, and low weight, aluminum (Al) and its alloys are an important class of engineering materials with many applications in our daily life, including the aerospace and shipping industries, packaging, construction, transportation, and many household items [9,11-12,15]. These materials are metallically bonded and, therefore, intrinsically hydrophilic with a large value of surface tension ranging from hundreds to thousands dyne/centimeter. This makes achieving the

_____

*Corresponding author. E-mail: m.ghashghaee@ippi.ac.ir

superhydrophobicity on their surface be relatively difficult [2].

The recent research efforts in preparing super-hydrophobic surfaces have essentially focused on generating micro/nano-scale (dual) roughness and surface treatments with low surface-energy molecules [12]. Several techniques are available to create a rough surface, including sol-gel [16-17], colloidal template [11], solution-immersion [12, 18], layer-by-layer assembly [19-20], laser fabrication [11], etching [21], chemical and electrochemical deposition [10,22], lithography [19,23], chemical/physical vapor deposition [24-25], electrospinning [14,26], molding [27], solvent-mediated phase separation [27-28], anodic oxidization [28], and template-based extrusion [27]. The widely employed reactive molecules for the low surface-energy modification are normally the long-chain fatty acids and thiols, perfluorinated alkyl agents, alkyl/fluorinated organic silanes, polydimethylsiloxane polymers and combinations thereof [5,12,29]. The long-chain fatty acids are among the most effective modifiers owing to their low surface energy and their suitable chemisorptions ability thus forming stable carboxylate groups on the surface [12,30-31]. For instance, Wen *et al.* [32] showed the anti-icing behavior of Al alloy modified with dodecanoic (lauric) acid. An ultrahydrophobic porous alumina surface with a water contact angle value of 154.2° was also prepared successfully *via* grafting an octadecanoic (stearic) acid film on a roughened Al substrate [33]. Zang *et al.* [8] reported the Al surface treatment using stearic acid as the modifier. Emphasizing the effect of the solvent ratio, these investigators could enhance the corrosion resistance and wettability of the Al surface, providing static contact angles of up to 167.3°. Another publication by Jafari and Farzaneh [5] reported the relatively high contact angle of ~154° and a CA hysteresis of about 30° through deposition of stearic acid layer on the Al alloy surface. The hydrophobic property was enhanced further by introducing SiO_2 and $CaCO_3$ nanoparticles and spraying the mixture on the surface. Consequently, high water contact angles of 162° and 158° and low contact angle hysteresis values of 3° and 5° were obtained, respectively, with the two mentioned additives. Some authors [9] reported a stable super-hydrophobic layer with a static contact angle of 154° after treatment of an anodized Al surface *via* chemisorption of myristic acid. The

authors also studied the change in the corrosion resistance and the surface stability. Other investigators showed [3] that the hydrophobicity can be fortified *via* tuning the morphology of the surface. An acceptably hydrophobic surface (a contact angle of ~150°) was achieved through the Al treatment with stearic acid alone, however.

The present work is aimed to explain the effect of individual steps in making an ultrahydrophobic Al surface including the cleaning/polishing, alkali treatment, acid washing, and modification with long-chain fatty acids. The effects of pivotal operating conditions including the time and temperature as well as the chemical factors such as the fatty acid and solvent are investigated for the first time.

EXPERIMENTAL

Aluminum sheets (containing Al, Mn, and Fe as the major elements) with 40 mm × 60 mm × 0.5 mm dimensions were employed as the alloy substrate. The aluminum plates were initially treated with a silicon carbide polisher (1200 grit) and cleaned with acetone. The cleaned plates were subsequently washed with deionized water for 5 min, immersed in a 1 M NaOH aqueous solution for 5 min, and dried at room temperature for 10 min. After the initial treatments, the samples were dipped in 2.6 M HCl solution for a certain time and finally rinsed with deionized water. The chemically treated sheets were modified by three fatty acids including stearic acid, oleic acid, and lauric acid. For this coating, the aluminum plates were immersed into the solution of fatty acid with a concentration of 0.005 M for 5 min at different temperatures. The tested solvents were acetone, toluene, water, dimethylformamide (DMF), and ethanol. The coated plates were finally dried in an oven at 75 °C for 45 min.
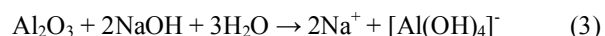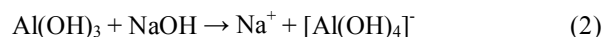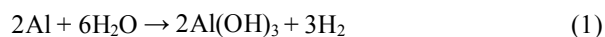
The attenuated total reflectance Fourier transform infrared (ATR-FTIR) spectra were obtained using on a Bruker Vertex 80 FTIR spectrometer. The surface morphology was explored using a TESCAN VEGA scanning electron microscope (SEM). For obtaining the static water contact angle of the plates, a water droplet of about 12 µl volume was placed on the surface through a needle and afterwards the image was captured with a digital camera within 30 s. Finally, the contact angles were

determined from the tangent line and the ellipse curve-fitting to the water droplet image using a Krüss G10 device. For the sliding angle, a droplet with the above-mentioned volume was placed on the surface and the slope of the surface with respect to the ground was increased until the droplet began to move. The angle obtained from the height of the surface at this moment was taken as the sliding angle. The elemental composition of the substrate was determined by a TESCAN VEGA3 SBU energy-dispersive X-ray spectroscopy (EDX) apparatus.

RESULTS AND DISCUSSION

Effects of the Preliminary Treatments on the Surface

The evolution of a superhydrophobic surface on the Al alloy during the initial steps is illustrated in Fig. 1 through consecutive molecular-scale images. Figure 1a shows the non-treated aluminum sheet. As implied by this panel, the surface of the alloy appears to be very smooth with no sizable hillocks. However, many corrugations become evident when the image is zoomed out to Fig. 1f. After polishing the surface (Fig. 1g), the corrugations of the surface at the larger scale disappeared almost entirely so that a uniform surface was prepared for the subsequent processing. Fig. 1b depicts the lower-scale effects which evinced an irregularity of the corrugations with respect to those in Fig. 1a. The next step involved the immersion in NaOH (1 M) solution (Fig. 1c). The main purpose of this treatment was to remove some of the Al oxide species on the surface, to facilitate the subsequent HCl etching process [8,34], and the oxidation of the surface [35-36]. The reactions involved in the said process are shown below [37]:

$$2Al + 6H_2O \rightarrow 2Al(OH)_3 + 3H_2 \tag{1}$$

$$Al(OH)_3 + NaOH \rightarrow Na^+ + [Al(OH)_4]^- \tag{2}$$

$$Al_2O_3 + 2NaOH + 3H_2O \rightarrow 2Na^+ + [Al(OH)_4]^- \tag{3}$$

The NaOH not only converts alumina moieties to the respective hydroxide species, but it also oxidizes the $Al(OH)_3$ species to hydroxide anions thus creating more hydroxyl groups on the surface. Clearly, the NaOH solution

also cleans the surface at high pH conditions and adequately high temperatures along with partial roughening of the surface [38]. As demonstrated in Fig. 1c, the immersion of the sheets in the sodium hydroxide solution resulted in a very mild but distributed corrosion effect on the surface, pointing out to the start of an etching treatment by NaOH. The fine corroded points are difficult to spot in Fig. 1h. However, the corroded points are more visible and plentiful in Fig. 1i due to the more severe etching of the surface in HCl solution according to the following equation [37]:

$$Al + HCl \rightarrow H_2 + AlCl_3 \tag{4}$$

As can be seen in Fig. 1d, the result of this etching process is the creation of many nano- and micro-sized cavities and hillocks on the surface, which are able to trap the air inside thus increasing the water contact angle and the hydrophobic property. The abundance and size of the cavities are two important parameters in producing the hydrophobicity. Figure 1j shows the Al sheets after the modification by stearic acid. The uniform spreading of a thin white layer of stearic acid on the surface is obvious in both panels of (e) and (j) in Fig. 1.

The chemical composition of the samples at each step was found using EDX analysis. The typical atomic percentage contents of the elements are given in Table 1. Up to the depth of ~3 μm which is analyzed by the EDX technique [39-42], elements such as Al, Fe, and Mn and their oxide species were present in the Al sheet as shown in Table 1. After surface polishing (sample 2), the composition of the surface did not change significantly. However, the Fe element and its oxide compounds disappeared from the composition. When the sample underwent immersion in sodium hydroxide (sample 3), the amount of oxygen increased substantially. This is an indication of the surface oxidation and creation of new hydroxyl groups on the surface. The NaOH treatment led to the introduction of 5.1% of Na onto the surface. However, the deposited Na disappeared upon subsequent processing in HCl solution as its chloride salt. The immersion of the plates in HCl commences the etching process, which is deemed to remove the previously formed metal oxide species from the surface through reduction, *e.g.*, to $AlCl_3$ moieties thus reducing the oxygen content of the surface. A small amount (0.2%) of
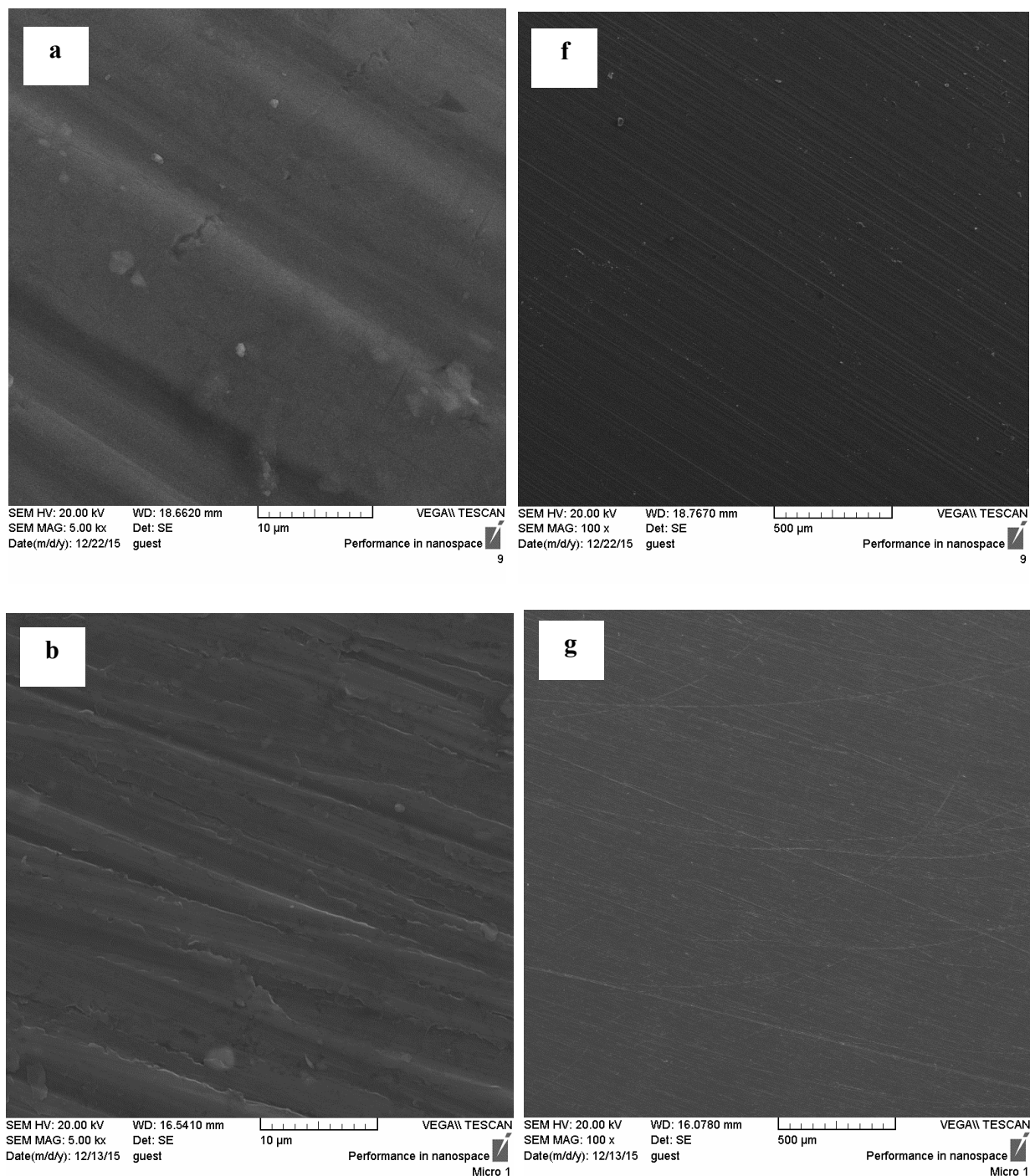
Fig. 1. SEM images of Al plates at two different magnifications of 10 μm (a-e) and 500 μm (f-j) where panels (a) and (f) related to the original non-treated surface, (b) and (g) to the polished surface, (c) and (h) to that further pretreated by NaOH, (d) and (i) to that chemically treated in HCl, and (e) and (j) to the sample modified by stearic acid.
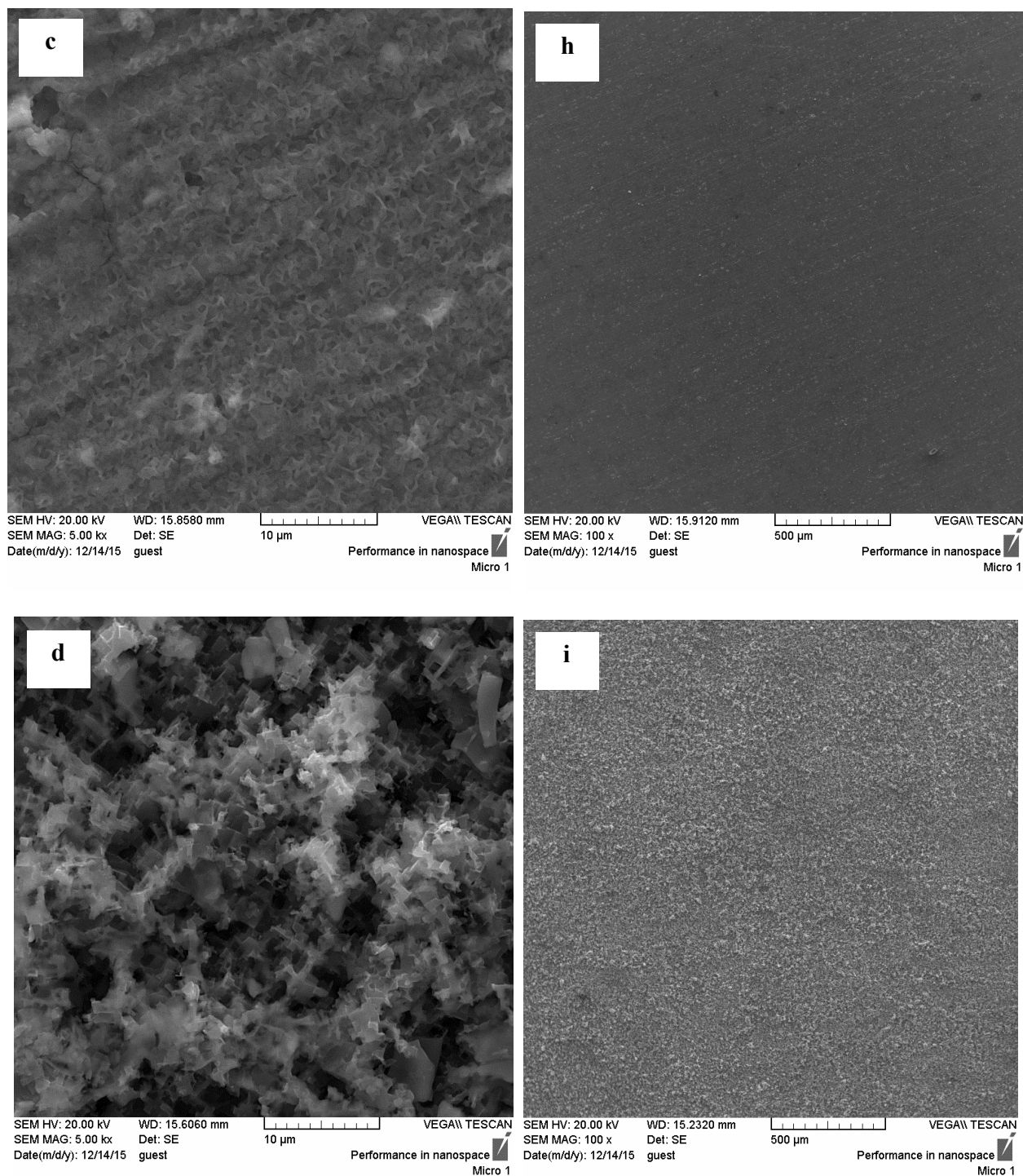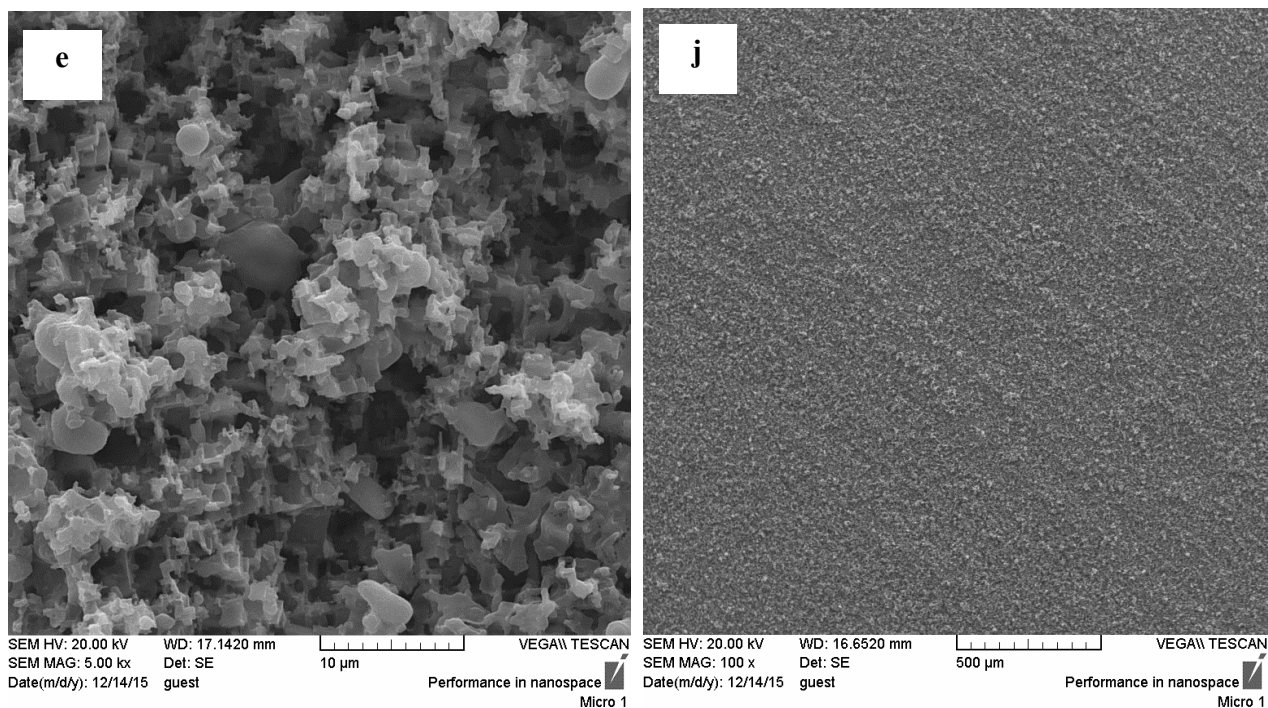
Fig. 1. Continued.

Fig. 1. Continued.

Table 1. Chemical Compositions of the Substrate at Different Steps Where Sample 1 Refers to the Original Non-treated Surface, Sample 2 to the Polished Surface, Sample 3 to the Substrate Further Pretreated by NaOH, Sample 4 to that Etched in HCl, and Sample 5 to the Substrate Modified by Stearic Acid

Elements	Sample 1	Sample 2	Sample 3	Sample 4	Sample 5
Al	93.66	90.38	42.76	66.92	41.64
Mn	0.22	0.44	0.23	0.37	0.18
O	5.84	9.19	51.96	32.50	20.08
Fe	0.27	0.00	0.00	0.00	0.00
Na	0.00	0.00	5.05	0.00	0.00
Cl	0.00	0.00	0.00	0.21	0.11
Si	0.00	0.00	0.00	0.00	0.36
C	0.00	0.00	0.00	0.00	37.64

Table 2. Water Static Contact Angles and Sliding Angles of the Al Sheet with Different Immersion Times of HCl Treatment at 20 °C. The Stearic Acid Modification was Implemented at 20 °C for 5 min

Immersion time (min)	2	5	10
Water contact angle	143.2°	157.3°	154.0°
Contact angle hysteresis	Too high	1.5°	1°

chlorine was also detectable on the surface (sample 4) after the HCl treatment. The appearance of carbon in EDX spectra for the samples after the last step (sample 5) demonstrates the reaction between aluminum surface and stearic acid.

Influence of Immersion Time in HCl on Superhydrophobic Property

Here, we discuss the effect of the HCl treatment duration (the etching time) on the water contact angle of the aluminum plates modified by stearic acid. As can be seen in Table 2, the optimum value for the time of immersion is about 5 min. Before this critical time, the contact angle is even as small as 143°, while above the peak time, the contact angle again reduces to 154°. In agreement with the SEM images, this indicates that a treatment in hydrochloric acid plays a vital role in creating the ultrahydrophobicity and self-cleaning properties. The chemical etching is believed [43] to increase the molecular-scale roughness on the surface which increases the hydrophobicity of the substrate accordingly. Indeed, the etching process generates hillocks and valleys on the surface, which in turn provide micrometer spaces to trap the air in between, leading to increased contact angles. When the etching time increases from ~5 min to 10 min, however, the mentioned terrains are postulated to be partially destroyed thus becoming poor in perfectly trapping the air inside [43]. Consequently, the contact angle is again decreased. Considering the curvature of the trends, therefore, the results indicated that an approximate time of 5-6 min is the optimal time for the etching process on the Al plates.

As observed in Table 2, the etching time has a great influence on the sliding angle as well. For a 2 min immersion time, the sample had a relatively good contact angle but had a very high sliding angle such that the water droplet could not slide down even a vertical surface. However, the immersion times of 5 and 10 min were long enough in providing considerably low sliding angle values. In fact, if suitable roughness is created on the surface, the cavities can trap the air and form a solid-air-liquid composite explained as the Cassie-Baxter state [7,44-45]. When the water droplet is in Cassie-Baxter state, the total contact area between the droplet and the solid surface is decreased and the adhesive force at their interface is weakened in such a manner that the water droplets roll off easily the surface and the tilt angle is decreased accordingly [46].

Effect of Reaction Temperature on Superhydrophobic Property

The effect of the reaction temperature on the contact angle of the resulting surface is discussed here. To our knowledge, this factor has not been investigated by other research groups. In a similar system of stearic acid in acetone at 30 °C, however, the contact angle measurements were done at temperatures ranging from -10-20 °C [5] where it was found that the Al alloy became less hydrophobic at supercooled temperatures. The authors did not report any change in the reaction temperature. Figure 2 contains the results of static contact angle and sliding angle at different reaction temperatures in the surface modification with stearic acid. As the reaction temperature is increased, the reaction energy for the hydrogen binding interaction is more conveniently provided such that the fatty
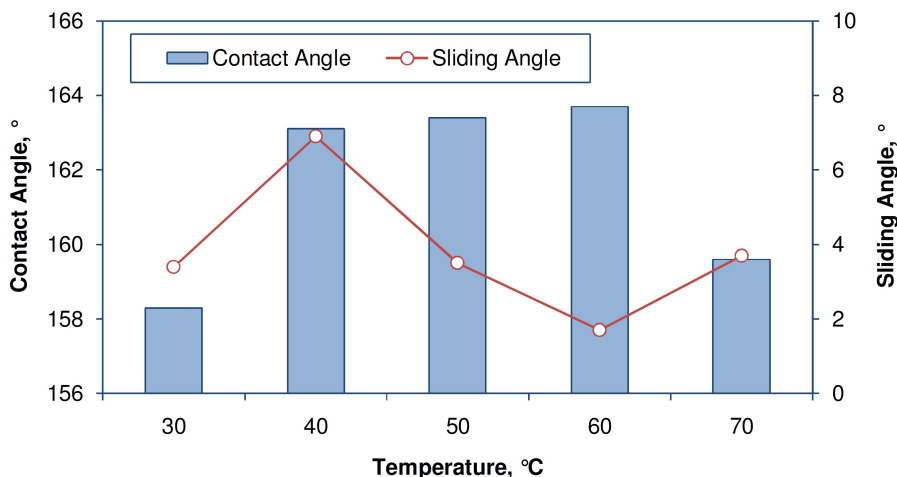
Fig. 2. Static contact angles and sliding angle of the samples after HCl treatment at different temperatures for 5 min.
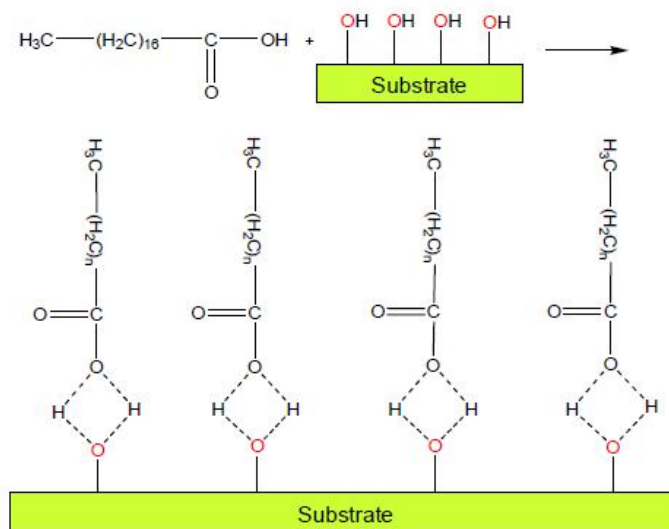

Fig. 3. The proposed mechanism for the reaction between the fatty acid molecules and the Al alloy surface.

acid could react more favorably with the Al substrate. The plausible binding mechanism is shown in Fig. 3. Overall, the reaction temperature of 60 °C was found to be optimal temperature with respect to both static contact angle and sliding angle. When the temperature was increased from 60 to 70 °C which was closer to the boiling point of ethanol, fast evaporation of ethanol occurred and, hence, deposition of the fatty acid was uncontrolled. This inevitably led to reduced contact angle at 70 °C compared to that at 60 °C. Other possible reasons for this observation include the weak interaction of the carboxylic group with the surface and the easy cleavage of the anchoring bonds due possibly to the high mobility of stearic acid in the solution at temperatures approaching its melting point.

As demonstrated in Fig. 2, the sliding angle was also measured for the samples. At the experimental conditions,
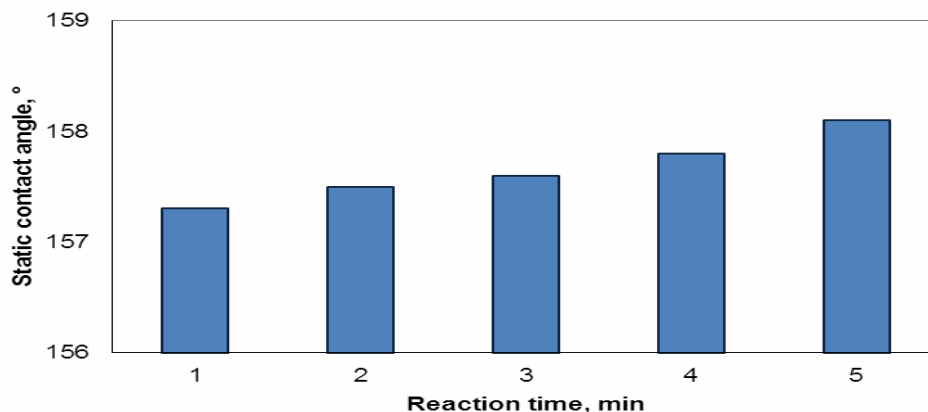
346

Fig. 4. Relationship between the water contact angle and the reaction time in surface modification with stearic acid at 20 °C. The samples had undergone HCl treatment at 20 °C for 5 min before the stearic acid modification.

all of the samples possessed a sliding angle being well lower than 7°. This indicated a good self-cleaning property for all of the modified plates. The alteration of the sliding angle with the reaction temperature exhibited no distinct trend owing probably to surface heterogeneities that influenced the sliding of the droplet on the surface.

Effect of Reaction Time between Stearic Acid and Aluminum Surface

Figure 4 shows the changes in the contact angle of water on the aluminum surface for varying reaction times at 20 °C. The obtained contact angles were above 157° indicating that all of the samples had an ultrahydrophobic property. This means that a 5 min modification in stearic acid is sufficient for creating an ultrahydrophobic Al surface. As the time increases, however, the water contact angle increases gradually with a mild rate. Although the prolonged processing with stearic acid would be advantageous, it will not be cost effective in industrial practice to employ long times. In general, it is anticipated that by increasing the reaction time, the surface energy of the substrate decreases thus increasing the contact angle. In a close study, *e.g.,* Yin *et al.* [47] measured the contact angle of water on aluminum surface under various processing times; the authors observed analogously that the contact angle increased upon prolonging the reaction time between the Al surface and perfluoroalkyltriethoxysilanes.

In another work by Ren *et al.* [48] in this respect, the investigators evaluated the contact angle of flat and rough Al surfaces modified by stearic acid at different reaction times. The obtained results for both of the samples showed increasing contact angles upon prolonging the reaction time. The slope of this rising trend decreased after ~10 h, however.

As demostrate in Table 3, the values of sliding angles of all of the samples were less than 6°. Therefore, all of samples had a satisfactory self-cleaning feature. Overall, the stearic acid modification increased the surface hydrophobicity with respect to the samples without this treatment (see the data in Figs. 2 and 4 for comparison).

Effect of Different Fatty Acids on Static Contact Angle and Sliding Angle

Figure 5 depicts the water droplets on the Al surfaces modified by three fatty acids. The FT-IR spectra of the aluminum surfaces modified by different fatty acids including stearic acid, lauric acid, and oleic acid are shown in Fig. 6. The FT-IR spectrum of the stearic-acid-modified sample (Fig. 7a) shows strong peaks at 2891 and 2825 cm^{-1}, assigned to the C-H asymmetric and symmetric stretching of aliphatic CH_2 groups, respectively [49]. The appearance of the mentioned peaks indicates the existence of long-chain alkyl groups on the aluminum surface.

The peak obtained at 1709 cm^{-1} could be attributed to

Table 3. Sliding Angles of the Samples after Stearic Acid Modification at Different Reaction Times at 20 °C. The Samples were under HCl Treatment at 20 °C for 5 min before the Stearic Acid Modification

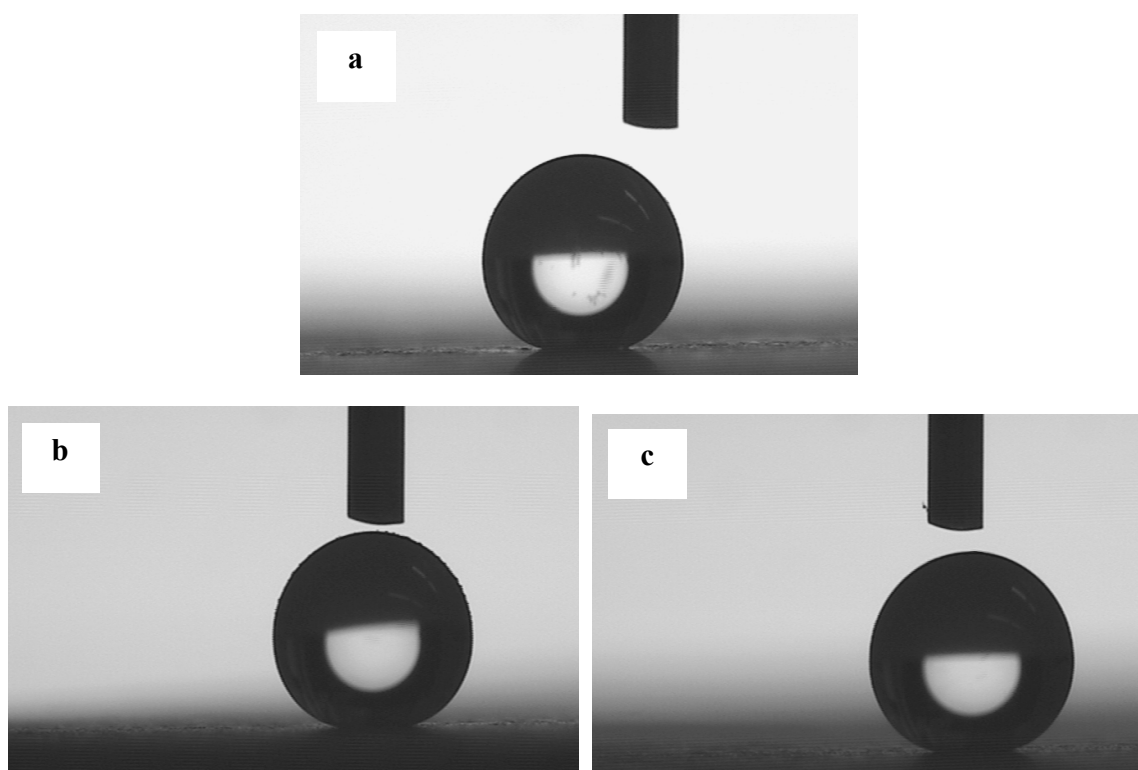| Reaction time (min)	5	10	15	20	25
Sliding angle	1.5°	2.4°	3.9°	5.7°	1.8°

Fig. 5. Typical images of water droplet on aluminum alloy samples modified by (a) stearic acid, (b) lauric acid, and (c) oleic acid.

the vibration of the carboxylic acid C=O bonds [50-51]. These altogether point out to the grafting of stearic acid onto the aluminum surface. The IR spectrum shown in Fig. 6b for the lauric acid modification indicates the regions of stretching frequencies identical to those observed for stearic acid except for their intensities. The reason behind this difference would be the fact that stearic acid contains six more carbon atoms compared to lauric acid. It might be due to a relatively lower amount of lauric acid chemisorbed on the Al surface. Figure 6c depicts the IR spectrum for the case of oleic acid modification. The peaks associated with the C-H bonds appeared at 2891 and 2825 cm^{-1} and that of C=O at 1709 cm^{-1}. For all of the samples, C-O stretching frequency was found at 1594 cm^{-1} [52] and the peak due to
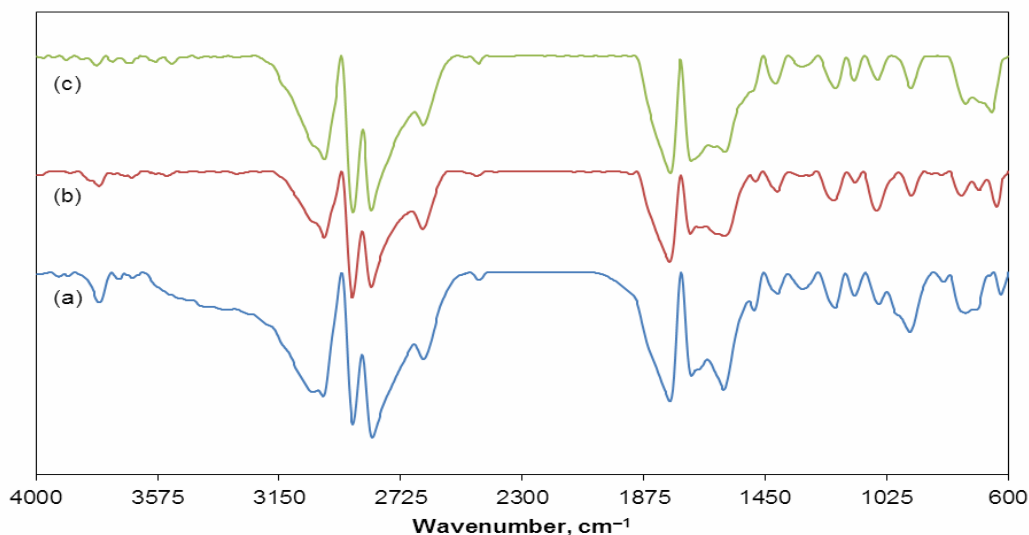
Fig. 6. FTIR-ATR spectra of aluminum surfaces modified by organic thin films of (a) stearic acid, (b) lauric acid, and (c) oleic acid.

Table 4. Static Contact Angles and Sliding Angle Values of Al Surfaces with Different Fatty Acids at Two Different Temperatures

	Temperature (°C)	Water contact angle (°)	Sliding angle (°)
Stearic acid	20	157.3	1.5
	60	163.7	1.7
Lauric acid	20	160.6	2.5
	60	157.0	3.3
Oleic acid	20	160.7	4.2
	60	159.5	3.9

the C-H bonding of CH_3 groups appeared at 2995 cm^{-1} [5]. In total, the IR spectra presented here demonstrated the adsorption of fatty acids on the aluminum surface albeit with low concentrations.

It is helpful to compare different fatty acids in modification of the Al surface. Three different fatty acids including stearic acid, oleic acid, and lauric acid were chosen to probe effect of the number of carbon atoms and carbon-carbon double bonds on the hydrophobicity. As observed in Fig. 7, stearic acid is a fatty acid with 18 carbon atoms with all of bonds being C-C except the carboxylic acid group. The structure of oleic acid is very similar to that of stearic acid but it is a monounsaturated omega-9 fatty acid with a lipid number of 18:1 cis-9 [53]. Lauric acid is also similar to stearic acid but having 6 less carbon atoms with respect to stearic acid.
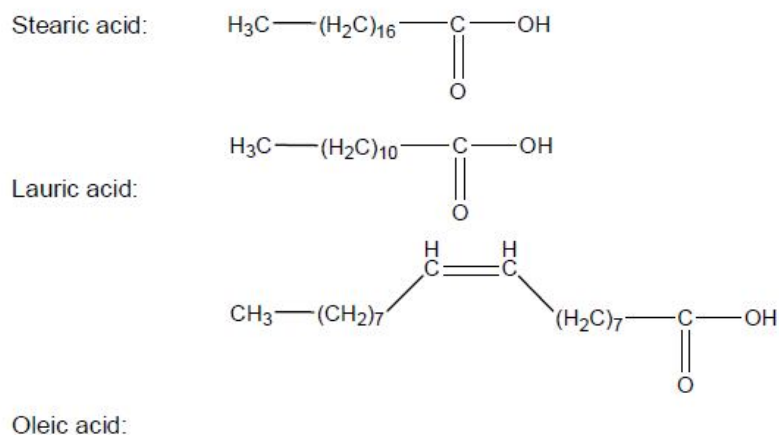
Stearic acid: H₃C——(H₂C)₁₆——C——OH ‖ O

Lauric acid: H₃C——(H₂C)₁₀——C——OH ‖ O

Oleic acid: CH₃——(CH₂)₇——CH=CH——(H₂C)₇——C——OH ‖ O

Fig. 7. Chemical structures of stearic acid, lauric acid and oleic acid.

Table 5. Static Water Contact Angles and Sliding Angle Values of Different Surfaces Modified by Stearic Acid at 60 °C and 5 min Using Different Solvents

Solvent	Acetone	Toluene	Water	DMF	Ethanol
Water contact angle	157.4°	<90°	152.3°	149.8°	163.7°
Sliding angle	12.0°	Failed	Failed	12.7°	1.7°

Table 6. Chemical Compositions of the Substrates after Modification by Stearic Acid at 60 °C for 5 min Using Different Solvents

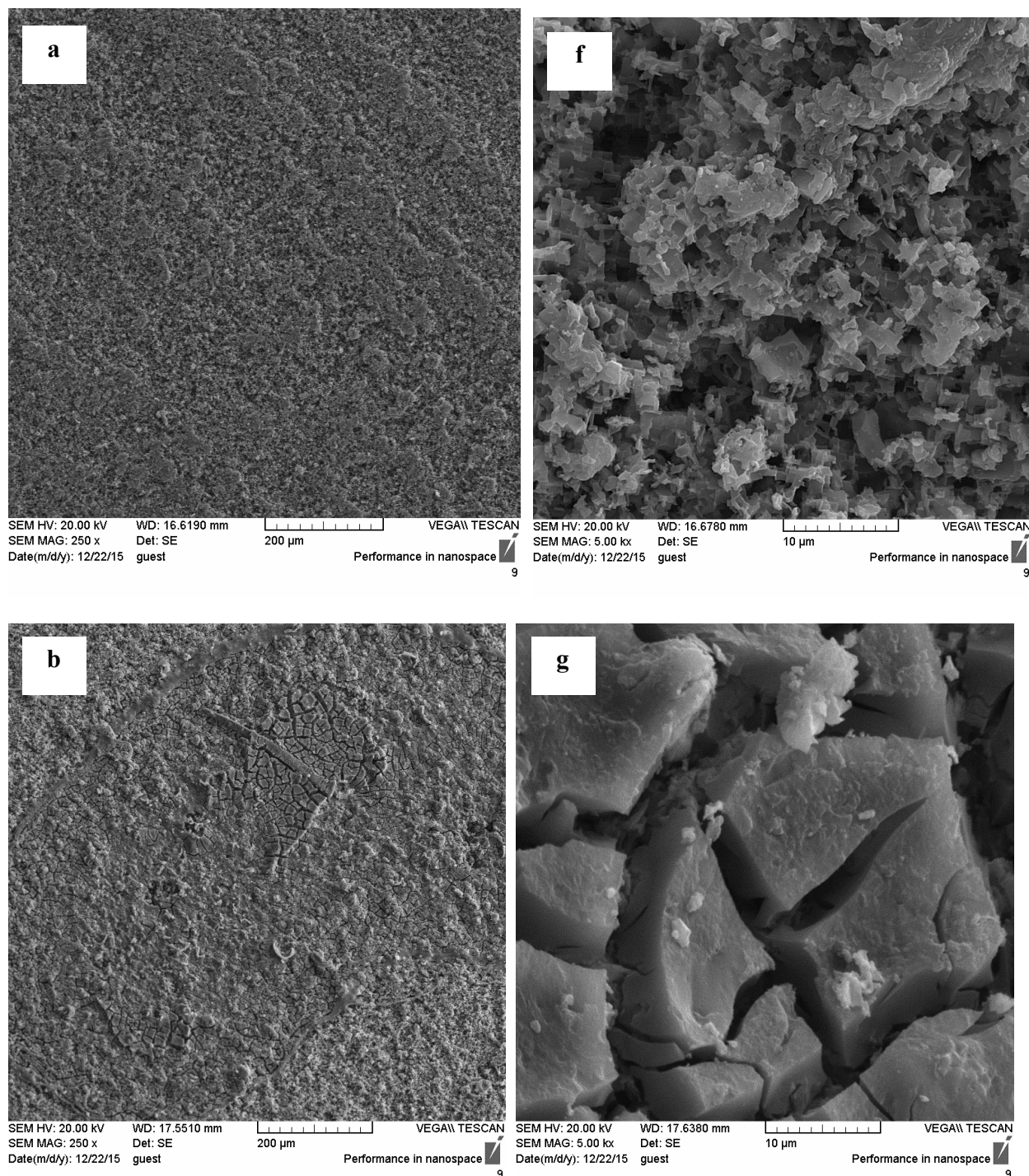| Elements	Acetone	Toluene	Water	DMF	Ethanol
Al	49.34	22.71	38.68	55.58	41.64
Mn	0.20	0.01	0.08	0.23	0.18
O	11.50	61.61	35.58	10.62	20.08
Fe	0.28	0.08	0.15	0.32	0
Na	0	0	0	0	0
Cl	0	1.20	0	0.58	0.11
Si	0.44	0.16	0.25	0.43	0.36
C	38.25	14.23	25.25	32.25	37.64

Fig. 8. SEM images of Al plates at two different magnifications of 500 µm (a-e) and 50 µm (f-j) where panels (a) and (f) are related to the acetone solvent, (b) and (g) to toluene, (c) and (h) to water, (d) and (i) to DMF, and (e) and (j) to ethanol.
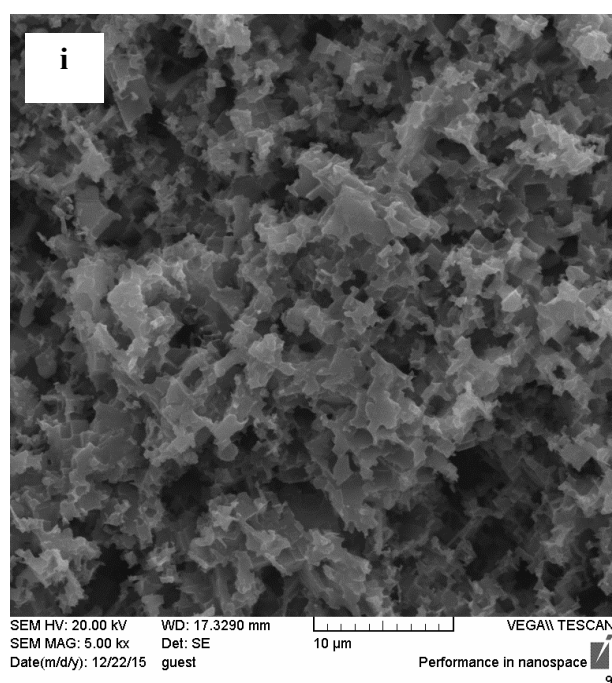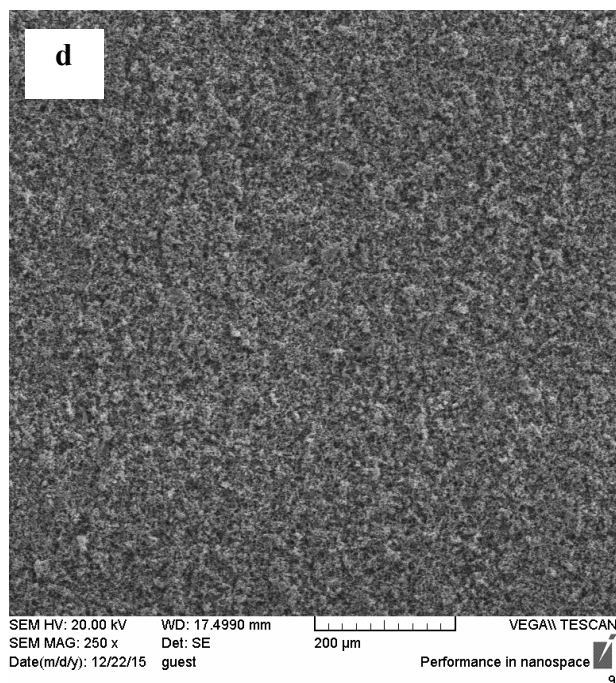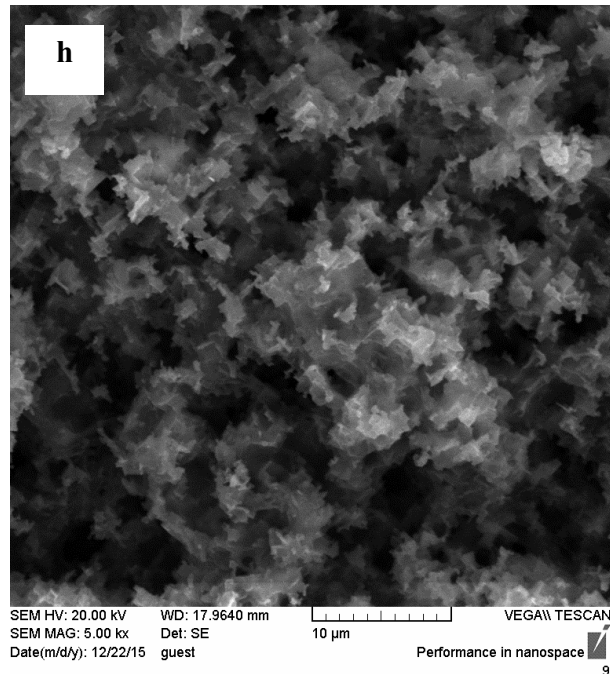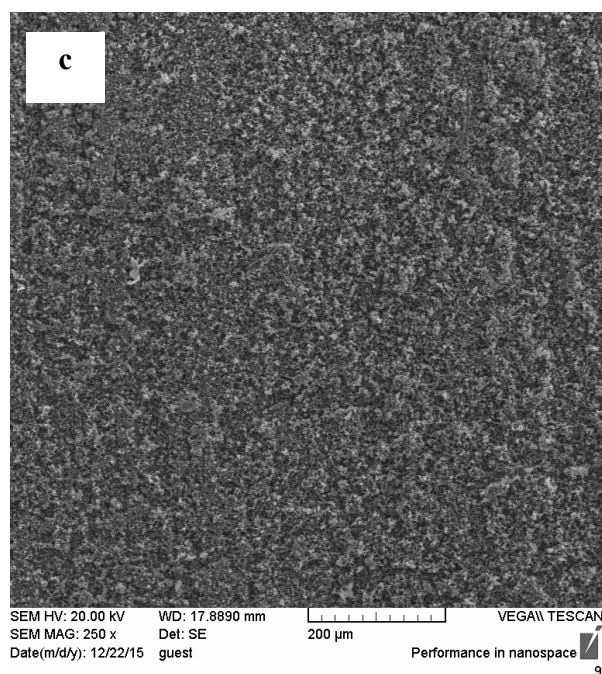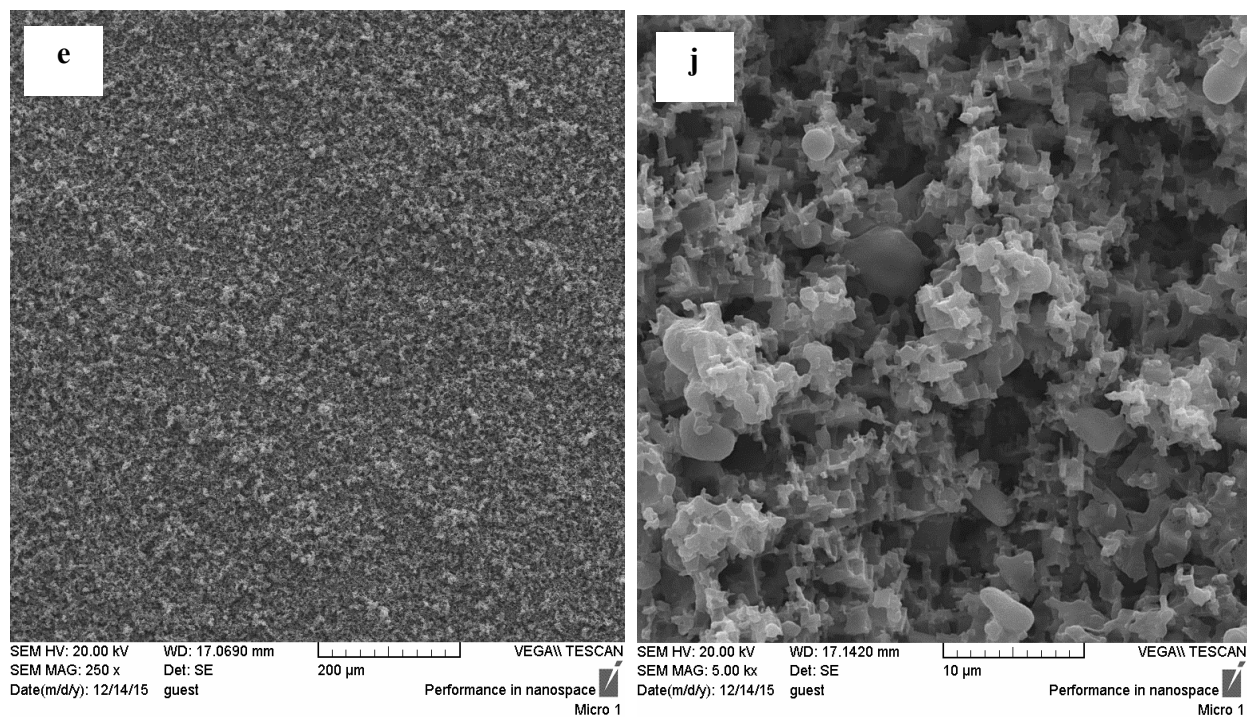
Fig. 8. Continued.

Fig. 8. Continued.

Overall, the three fatty acids showed similar behaviors in providing the hydrophobicity such that their corresponding sheets were all superhydrophobic (Table 4), though their behavior was different at the two temperature levels studied. At the reaction temperature of 20 °C, the contact angle with stearic acid modification was less than the other two fatty acids which were equally good at hydrophobization (showing contact angles of ~161°). In contrast to the low-temperature conditions, however, the stearic acid provided the highest contact angle (of about 164°) among the three fatty acids at 60 °C. This means that the static contact angle of stearic acid increased with increasing the reaction temperature while it decreased for the case of lauric acid and remained almost unchanged in the case of oleic acid modification. These findings would be considered as initial guidelines for any possible application in industry. As such, one would prefer using oleic acid as a modifying agent of low surface energy for the desired low-temperature conditions.

Effect of Different Solvents with Stearic Acid as the Surface Modifier

This part explains the effect of different solvents in the course of the modification with stearic acid in terms of the contact angle. A total of five solvents were used, including acetone, toluene, water, DMF and ethanol. As seen in Table 5, the static contact angle and sliding angle of the sample treated with stearic acid in ethanol was better than those in the other solvents. As a general observation, however, the obtained contact angle was high for most of the solvents (with the exception of toluene) such that the resulting surface was adequately hydrophobic. However, only ethanol gave a satisfactory sliding angle. For acetone and DMF, the contact angle was slightly higher than 10° but they have to be rejected because the self-cleaning feature is commonly attributed to surfaces with a sliding angle of lower than 10° [54]. With water and toluene as the solvent, the sliding angle was very high, thus being far from a self-cleaning ability. The toluene was the worst case as it did not lead to

any superhydrophobic property. To further probe these findings, we studied the samples also via SEM and EDX analyses. As demonstrated in Table 6, the amount of carbon on the surface, which is an indication of the stearic acid uptake of the surface, is about 38% in the case of ethanol and acetone solvents, being higher than the other solvents. The toluene-solvent case which exhibited a hydrophilic property possessed the lowest C percentage (~14%).

As also shown in Fig. 7, the deposition of the stearic acid over the surface is acceptable for all of the cases except for the toluene solvent in which the fatty acid covered the surface non-uniformly. Therefore, the toluene is not a suitable solvent for the reaction medium. The SEM images obtained with water as the solvent revealed some non-uniformity of the organic layer on the surface which is most probably the main reason for a high sliding angle in this case. Despite the lower C percentage on the surface treated in water than DMF (Table 6) and the less uniform layering of stearic acid in the former case (Fig. 8), the static contact angle of the surface prepared in water was slightly higher. This means that the layering of an organic compound might fulfill one aspect such as hydrophobicity while rejecting another property such as self-cleaning. Then, a perfect modification requires an adequately uniform deposition of the fatty acid on the surface without deteriorating the roughness of the surface. The ethanol at the first priority level acceptably provided these criteria for the Al sheets at the experimental conditions at hand, such that the high level of uniformity (Fig. 8) and the quality of the binding of stearic acid enabled a very low sliding angle (Table 5), meaning as a very good self-cleaning property.

CONCLUSIONS

In this article, we explained the steps of fabrication of a superhydrophobic aluminum surface coated with stearic acid, lauric acid, and oleic acid. We discussed the effects of several important factors influencing the contact angle and sliding angle. The resulting surface demonstrated a promising superhydrophobicity along with a satisfactory self-cleaning property. An about 5-min duration for the etching process and the reaction temperature of about 60 °C were found to be optimum conditions for the creation of a superhydrophobic surface with a self-cleaning feature. The

best results obtained at the optimum conditions were a contact angle of 163.7° and a sliding angle of about 1°. By increasing the reaction time, the contact angle increased with a small slope; however, an increase in the reaction time could not be reasonable from an economical point of view. Regarding the best results at near-ambient temperatures, the most appropriate fatty acid for the Al surface modification was oleic acid and the best solvent was ethanol. By addressing the important practical factors in the preparation steps, the present study can help in creating superhydrophobic aluminum surfaces with high contact angles and perfect self-cleaning properties through simple and low-cost procedures. Although, the results were obtained on Al plates, the trends and methods should be applicable to other systems. However, the optimum conditions may clearly differ from those reported in this article.

REFERENCES

[1] Gao, J.; Li, Y.; Li, Y.; Liu, H.; Yang, W., Fabrication of superhydrophobic surface of stearic acid grafted zinc by using an aqueous plasma etching technique. *Cent. Eur. J. Chem.* **2012**, *10*, 1766-1772, DOI: 10.2478/s11532-012-0116-0.

[2] Xie, D.; Li, W., A novel simple approach to preparation of superhydrophobic surfaces of aluminum alloys. *Appl. Surf. Sci.* **2011**, *258*, 1004-1007, DOI: 10.1016/j.apsusc.2011.07.104.

[3] Lv, Y. Z.; Wang, L. F.; Ma, K. B.; Zhou, Y.; Li, C. R., Fabrication of superhydrophobic films on aluminum foils with controllable morphologies. *Adv. Mat. Res.* **2013**, *641-642*, 414-417, DOI: 10.4028/www.scientific.net/AMR.641-642.414.

[4] Wankhede, R. G.; Shantaram, K. T.; Khanna, A.; Birbillis, N., Development of hydrophobic non-fluorine sol-gel coatings on aluminium using long chain alkyl silane precursor. *J. Mat. Sci. Eng. A* **2013**, *3*, 224-231.

[5] Jafari, R.; Farzaneh, M., A simple method to create superhydrophobic aluminium surfaces. *Mat. Sci. Forum* **2012**, *706-709*, 2874-2879, DOI: 10.4028/www.scientific.net/msf.706-709.2874.

[6] Mohamed, A. M. A.; Abdullah, A. M.; Younan, N.

A., Corrosion behavior of superhydrophobic surfaces: A review. *Arab. J. Chem.* **2015**, *8*, 749-765, DOI: 10.1016/j.arabjc.2014.03.006.

[7] Chen, Z.; Tian, F.; Hu, A.; Li, M., A facile process for preparing superhydrophobic nickel films with stearic acid. *Surf. Coat. Tech.* **2013**, *231*, 88-92, DOI: 10.1016/j.surfcoat.2012.01.053.

[8] Zang, D.; Zhu, R.; Zhang, W.; Wu, J.; Yu, X.; Zhang, Y., Stearic acid modified aluminum surfaces with controlled wetting properties and corrosion resistance. *Corros. Sci.* **2014**, *83*, 86-93, DOI: 10.1016/j.corsci.2014.02.003.

[9] Yin, Y.; Liu, T.; Chen, S.; Liu, T.; Cheng, S., Structure stability and corrosion inhibition of superhydrophobic film on aluminum in seawater. *Appl. Surf. Sci.* **2008**, *255*, 2978-2984, DOI: 10.1016/j.apsusc.2008.08.088.

[10] Huang, Y.; Sarkar, D. K.; Chen, X. G., Fabrication of superhydrophobic surfaces on aluminum alloy *via* electrodeposition of copper followed by electrochemical modification. *Nano-Micro Lett.* **2011**, *3*, 160-165, DOI: 10.1007/bf03353667.

[11] Liu, C.; Su, F.; Liang, J., Facile fabrication of a robust and corrosion resistant superhydrophobic aluminum alloy surface by a novel method. *RSC Adv.* **2014**, *4*, 55556-55564, DOI: 10.1039/c4ra09390a.

[12] Vengatesh, P.; Kulandainathan, M. A., Hierarchically ordered self-lubricating superhydrophobic anodized aluminum surfaces with enhanced corrosion resistance. *ACS Appl. Mater. Inter.* **2015**, *7*, 1516-1526, DOI: 10.1021/am506568v.

[13] Wang, F.; Shen, T.; Li, C.; Li, W.; Yan, G., Low temperature self-cleaning properties of superhydrophobic surfaces. *Appl. Surf. Sci.* **2014**, *317*, 1107-1112, DOI: 10.1016/j.apsusc.2014.08.200.

[14] Lu, S.; Chen, Y.; Xu, W.; Liu, W., Controlled growth of superhydrophobic films by sol-gel method on aluminum substrate. *Appl. Surf. Sci.* **2010**, *256*, 6072-6075, DOI: 10.1016/j.apsusc.2010.03.122.

[15] Qin, L.; Zhao, W.; Hou, H.; Jin, Y.; Zeng, Z.; Wu, X.; Xue, Q., Achieving excellent anti-corrosion and tribological performance by tailoring the surface morphology and chemical composition of aluminum alloys. *RSC Adv.* **2014**, *4*, 60307-60315, DOI:

10.1039/c4ra10112j.

[16] Yang, H.; Pi, P.; Cai, Z. -Q.; Wen, X.; Wang, X.; Cheng, J.; Yang, Z. -R., Facile preparation of super-hydrophobic and super-oleophilic silica film on stainless steel mesh *via* sol-gel process. *Appl. Surf. Sci.* **2010**, *256*, 4095-4102, DOI: 10.1016/j.apsusc.2010.01.090.

[17] Siriviriyanun, A.; Imae, T., Anti-fingerprint properties of non-fluorinated organosiloxane self-assembled monolayer-coated glass surfaces. *Chem. Eng. J.* **2014**, *246*, 254-259, DOI: 10.1016/j.cej.2014.02.066.

[18] Zhang, Y.; Wu, J.; Yu, X.; Wu, H., Low-cost one-step fabrication of superhydrophobic surface on Al alloy. *Appl. Surf. Sci.* **2011**, *257*, 7928-7931, DOI: 10.1016/j.apsusc.2011.03.096.

[19] Zhang, X.; Shi, F.; Niu, J.; Jiang, Y.; Wang, Z., Superhydrophobic surfaces: from structural control to functional application. *J. Mater. Chem.* **2008**, *18*, 621-633, DOI: 10.1039/b711226b.

[20] Zhang, M.; Wang, S.; Wang, C.; Li, J., A facile method to fabricate superhydrophobic cotton fabrics. *Appl. Surf. Sci.* **2012**, *261*, 561-566, DOI: 10.1016/j.apsusc.2012.08.055.

[21] Liao, R.; Zuo, Z.; Guo, C.; Yuan, Y.; Zhuang, A., Fabrication of superhydrophobic surface on aluminum by continuous chemical etching and its anti-icing property. *Appl. Surf. Sci.* **2014**, *317*, 701-709, DOI: 10.1016/j.apsusc.2014.08.187.

[22] Li, M.; Zhai, J.; Liu, H.; Song, Y.; Jiang, L.; Zhu, D., Electrochemical deposition of conductive superhydrophobic zinc oxide thin films. *J. Phys. Chem. B* **2003**, *107*, 9954-9957, DOI: 10.1021/jp035562u.

[23] Fürstner, R.; Barthlott, W.; Neinhuis, C.; Walzel, P., Wetting and self-cleaning properties of artificial superhydrophobic surfaces. *Langmuir* **2005**, *21*, 956-961, DOI: 10.1021/la0401011.

[24] Ishizaki, T.; Hieda, J.; Saito, N.; Saito, N.; Takai, O., Corrosion resistance and chemical stability of super-hydrophobic film deposited on magnesium alloy AZ31 by microwave plasma-enhanced chemical vapor deposition. *Electrochim. Acta* **2010**, *55*, 7094-7101, DOI: 10.1016/j.electacta.2010.06.064.

[25] Lau, K. K. S.; Bico, J.; Teo, K. B. K.; Chhowalla, M.;

Amaratunga, G. A. J.; Milne, W. I.; McKinley, G. H.; Gleason, K. K., Superhydrophobic carbon nanotube forests. *Nano Lett.* **2003**, *3*, 1701-1705, DOI: 10.1021/nl034704t.

[26] Wang, S.; Liu, Q.; Zhang, Y.; Wang, S.; Li, Y.; Yang, Q.; Song, Y., Preparation of a multifunctional material with superhydrophobicity, superparamagnetism, mechanical stability and acids-bases resistance by electrospinning. *Appl. Surf. Sci.* **2013**, *279*, 150-158, DOI: 10.1016/j.apsusc.2013.04.060.

[27] Wang, Q.; Zhang, B.; Qu, M.; Zhang, J.; He, D., Fabrication of superhydrophobic surfaces on engineering material surfaces with stearic acid. *Appl. Surf. Sci.* **2008**, *254*, 2009-2012, DOI: 10.1016/j.apsusc.2007.08.039.

[28] Lv, F. Y.; Zhang, P., Fabrication and characterization of superhydrophobic surfaces on aluminum alloy substrates. *Appl. Surf. Sci.* **2014**, *321*, 166-172, DOI: 10.1016/j.apsusc.2014.09.147.

[29] Richard, E.; Lakshmi, R. V.; Aruna, S. T.; Basu, B. J., A simple cost-effective and eco-friendly wet chemical process for the fabrication of superhydrophobic cotton fabrics. *Appl. Surf. Sci.* **2013**, *277*, 302-309, DOI: 10.1016/j.apsusc.2013.04.052.

[30] Liascukiene, I.; Steffenhagen, M.; Asadauskas, S. J.; Lambert, J. -F.; Landoulsi, J., Self-assembly of fatty acids on hydroxylated Al surface and effects of their stability on wettability and nanoscale organization. *Langmuir* **2014**, *30*, 5797-5807, DOI: 10.1021/la404756y.

[31] Lim, M. S.; Feng, K.; Chen, X.; Wu, N.; Raman, A.; Nightingale, J.; Gawalt, E. S.; Korakakis, D.; Hornak, L. A.; Timperman, A. T., Adsorption and desorption of stearic acid self-assembled monolayers on aluminum oxide. *Langmuir* **2007**, *23*, 2444-2452, DOI: 10.1021/la061914n.

[32] Ruan, M.; Li, W.; Wang, B.; Deng, B.; Ma, F.; Yu, Z., Preparation and anti-icing behavior of superhydrophobic surfaces on aluminum alloy substrates. *Langmuir* **2013**, *29*, 8482-8491, DOI: 10.1021/la400979d.

[33] Feng, L.; Zhang, H.; Mao, P.; Wang, Y.; Ge, Y., Superhydrophobic alumina surface based on stearic acid modification. *Appl. Surf. Sci.* **2011**, *257*, 3959-3963, DOI: 10.1016/j.apsusc.2010.11.143.

[34] Awad, S. A.; Kamel, K. H. M.; Kassab, A., Corrosion behaviour of aluminium in NaOH solutions. *J. Electroanal. Chem. Inter. Electrochem.* **1979**, *105*, 291-294, DOI: 10.1016/S0022-0728(79)80123-0.

[35] Wu, R. M.; Liang, S. Q.; Chen, H.; Pan, A. Q.; Jiang, H. Y.; Deng, J.; Yu, Y.; Yuan, Z. Q.; Liu, Q. L., Fabrication of a super-hydrophobic micro-nanoporous aluminum surface by anodic oxidation. *Appl. Mech. Mater.* **2012**, *200*, 190-193, DOI: 10.4028/www.scientific.net/AMM.200.190.

[36] Lopez, K., Hierarchical superhydrophobic aluminum surfaces for condensation applications. BSc thesis, Massachusetts Institute of Technology: 2012.

[37] Kiyokazu, Y.; Ryo, S., Effect of surface roughening of aluminum plates on the strength of bonds formed between aluminum and polyphenylene sulfide by thermosonic bonding. *IOP Conf. Ser. Mater. Sci. Eng.* **2014**, *61*, 012007-1-012007-6, DOI: 10.1088/1757-899X/61/1/012007.

[38] Saleema, N.; Sarkar, D.; Paynter, R.; Chen, X. -G., Superhydrophobic aluminum alloy surfaces by a novel one-step process. *ACS Appl. Mater. Inter.* **2010**, *2*, 2500-2502, DOI: 10.1021/am100563u.

[39] Scheithauer, U., Application of the analytical methods REM/EDX, AES and SNMS to a chlorine induced aluminium corrosion. *Fresenius J. Anal. Chem.* **1991**, *341*, 445-448, DOI: 10.1007/BF00321954.

[40] Evans Analytical Group, EAGLABS Scanning Electron Microscopy (SEM)/Energy Dispersive X-ray Spectroscopy (EDS) Services. Evans Analytical Group: 2009, http://www.eag.com.

[41] Material Interface, Scanning Electron Microscopy (SEM) with Energy Dispersive X-Ray Analysis (EDX). Material Interface, Inc.: 2016, http://www.lucideon.com/testing-analysis/techniques/sem-edx.

[42] Vrije Universiteit Brussel, Scanning Electron Microscopy & Energy Dispersive X-Ray Spectroscopy. Vrije Universiteit Brussel: 2016, http://www.surfgroup.be/semedx.

[43] Chen, Z.; Guo, Y.; Fang, S., A facial approach to fabricate superhydrophobic aluminum surface. *Surf. Interface Anal.* **2010**, *42*, 1-6, DOI: 10.1002/sia.3126.

[44] Miwa, M.; Nakajima, A.; Fujishima, A.; Hashimoto, K.; Watanabe, T., Effects of the surface roughness on sliding angles of water droplets on superhydrophobic surfaces. *Langmuir* **2000**, *16*, 5754-5760, DOI: 10.1021/la991660o.

[45] Nosonovsky, M.; Bhushan, B., Chapter 2. Lotus Versus Rose: Biomimetic Surface Effects. in: Nosonovsky, M.; Bhushan, B. (Eds.), Green Tribology, Green Energy and Technology. Springer-Verlag Berlin Heidelberg: 2012, pp. 25-40, DOI: 10.1007/978-3-642-23681-5_2.

[46] Sanjay, S. L.; Annaso, B. G.; Chavan, S. M.; Rajiv, S. V., Recent progress in preparation of superhydrophobic surfaces: a review. *J. Surf. Eng. Mater. Adv. Tech.* **2012**, *2*, 76-94, DOI: 10.4236/ jsemat.2012.22014.

[47] Yin, L.; Wang, Y.; Ding, J.; Wang, Q.; Chen, Q., Water condensation on superhydrophobic aluminum surfaces with different low-surface-energy coatings. *Appl. Surf. Sci.* **2012**, *258*, 4063-4068, DOI: 10.1016/ j.apsusc.2011.12.100.

[48] Ren, S.; Yang, S.; Zhao, Y.; Yu, T.; Xiao, X., Preparation and characterization of an ultrahydrophobic surface based on a stearic acid self-assembled monolayer over polyethyleneimine thin films. *Surf. Sci.* **2003**, *546*, 64-74, DOI: 10.1016/ j.susc.2003.09.018.

[49] Wang, C.; Zhang, M.; Xu, Y.; Wang, S.; Liu, F.; Ma, M.; Zang, D.; Gao, Z., One-step synthesis of unique silica particles for the fabrication of bionic and stably superhydrophobic coatings on wood surface. *Adv. Powder Technol.* **2014**, *25*, 530-535, DOI: 10.1016/ j.apt.2013.08.007.

[50] Li, Z. W.; Ma, H. C.; Wang, J.; Zhang, Z. J., Preparation of hydrophobic magnesium hydroxide nanoparticles by oleic acid and polystyrene-grafting surface modification. *Adv. Mat. Res.* **2013**, *643*, 191-194, DOI: 10.4028/www.scientific.net/AMR.643.191.

[51] Vo, D. Q.; Kim, E.-J.; Kim, S., Surface modification of hydrophobic nanocrystals using short-chain carboxylic acids. *J. Colloid Interf. Sci.* **2009**, *337*, 75-80, DOI: 10.1016/j.jcis.2009.04.078.

[52] Rezayi, T.; Entezari, M. H., Toward a durable superhydrophobic aluminum surface by etching and ZnO nanoparticle deposition. *J. Colloid Interf. Sci.* **2016**, *463*, 37-45, DOI: 10.1016/j.jcis.2015.10.029.

[53] Wikipedia contributors, Oleic acid. Wikipedia, The Free Encyclopedia: 2016.

[54] Lee, H.; Bhushan, B., Fabrication and characterization of hierarchical nanostructured smart adhesion surfaces. *J. Colloid Interf. Sci.* **2012**, *372*, 231-238, DOI: 10.1016/j.jcis.2012.01.020.